



Chemical Bond Energies of 3d Transition Metals Studied by Density Functional Theory

Moltved, Klaus A.d; Kepp, Kasper P.

Published in:
Journal of Chemical Theory and Computation

Link to article, DOI:
[10.1021/acs.jctc.8b00143](https://doi.org/10.1021/acs.jctc.8b00143)

Publication date:
2018

Document Version
Peer reviewed version

[Link back to DTU Orbit](#)

Citation (APA):
Moltved, K. A. D., & Kepp, K. P. (2018). Chemical Bond Energies of 3d Transition Metals Studied by Density Functional Theory. *Journal of Chemical Theory and Computation*, 14(7), 3479-3492.
<https://doi.org/10.1021/acs.jctc.8b00143>

General rights

Copyright and moral rights for the publications made accessible in the public portal are retained by the authors and/or other copyright owners and it is a condition of accessing publications that users recognise and abide by the legal requirements associated with these rights.

- Users may download and print one copy of any publication from the public portal for the purpose of private study or research.
- You may not further distribute the material or use it for any profit-making activity or commercial gain
- You may freely distribute the URL identifying the publication in the public portal

If you believe that this document breaches copyright please contact us providing details, and we will remove access to the work immediately and investigate your claim.

Chemical Bond Energies of 3d Transition Metals Studied by Density Functional Theory

Klaus August Moltved, and Kasper P. Kepp

J. Chem. Theory Comput., **Just Accepted Manuscript** • DOI: 10.1021/acs.jctc.8b00143 • Publication Date (Web): 29 May 2018

Downloaded from <http://pubs.acs.org> on June 4, 2018

Just Accepted

"Just Accepted" manuscripts have been peer-reviewed and accepted for publication. They are posted online prior to technical editing, formatting for publication and author proofing. The American Chemical Society provides "Just Accepted" as a service to the research community to expedite the dissemination of scientific material as soon as possible after acceptance. "Just Accepted" manuscripts appear in full in PDF format accompanied by an HTML abstract. "Just Accepted" manuscripts have been fully peer reviewed, but should not be considered the official version of record. They are citable by the Digital Object Identifier (DOI®). "Just Accepted" is an optional service offered to authors. Therefore, the "Just Accepted" Web site may not include all articles that will be published in the journal. After a manuscript is technically edited and formatted, it will be removed from the "Just Accepted" Web site and published as an ASAP article. Note that technical editing may introduce minor changes to the manuscript text and/or graphics which could affect content, and all legal disclaimers and ethical guidelines that apply to the journal pertain. ACS cannot be held responsible for errors or consequences arising from the use of information contained in these "Just Accepted" manuscripts.



Chemical Bond Energies of 3d Transition Metals Studied by Density Functional Theory

Klaus A. Moltved and Kasper P. Kepp*

Technical University of Denmark, DTU Chemistry, Building 206, 2800 Kgs. Lyngby, DK – Denmark. *Phone: +045 45 25 24 09. E-mail: kpj@kemi.dtu.dk

Abstract. Despite their vast importance to inorganic chemistry, materials science and catalysis, the accuracy of modelling the formation or cleavage of metal-ligand (M-L) bonds depends greatly on the chosen functional and the type of bond in a way that is not systematically understood. In order to approach a state of high-accuracy DFT for rational prediction of chemistry and catalysis, such system-dependencies need to be resolved. We studied 30 different density functionals applied to a “balanced data set” of 60 experimental diatomic M-L bond energies; this data set has no bias toward any d^q configuration, metal, bond type, or ligand as all of these occur to the same extent, and we can therefore identify accuracy bottlenecks. We show that the performance of a functional is very dependent on data set choice and we dissect these effects into system type. In addition to the use of balanced data sets, we also argue that the precision (rather than just accuracy) of a functional is of interest, measured by standard deviations of the errors. There are distinct system dependencies both in the ligand and metal series: Hydrides are best described by a very large HF exchange percentage, possibly due to self-interaction error, whereas halides are best described by very small (0-10%) HF exchange fractions, and double-bond enforcing oxides and sulfides favor 10-25% HF exchange, as is also average for the full data set. Thus, average HF requirements hide major system-dependent requirements. For late transition metals Co-Zn, HF percentage of 0-10% is favored, whereas the early transition metals Sc-Fe hybrid functionals with 20% HF exchange or higher is commonly favored. Accordingly, B3LYP is an excellent choice for early d-block but a poor choice for late transition metals. We conclude

that DFT intrinsically underestimates the bond strengths of late vs. early transition metals, correlating with increased effective nuclear charge. Thus, the revised RPBE, which reduces the over-binding tendency of PBE, is mainly an advantage for the early-mid transition metals and not very much for the late transition metals, i.e. there is a metal-dependent effect of the relative performance of RPBE vs. PBE, which are widely used to study adsorption energetics on metal surfaces. Overall, the best performing functionals are PW6B95, the MN15 and MN15-L functionals, and the double hybrid B2PLYP.

Keywords: DFT, metal-ligand bond, Hartree-Fock exchange, accuracy, bond dissociation energy.

Introduction.

Understanding the chemical bond in its various manifestations is an essential task of chemistry. While the chemical bond is in principle completely described by quantum mechanics, in practice it requires the computation by quantum chemistry methods. Metal-ligand bonds (M-L) play a prominent role in many chemical reactions, and many endeavors in catalysis and inorganic chemistry depend directly on our ability to understand and manipulate such bonds.

Kohn-Sham density functional theory (referred to as DFT below) is today the most used method in computational quantum chemistry¹. The development of accurate gradient-corrected functionals and the introduction of some Hartree-Fock exchange in hybrids have been critical steps towards higher accuracy^{2,3}. Many currently used density functionals have been parametrized toward data for main-group molecules with single-determinant wave functions⁴. The B3LYP⁵ functional is the most widely used hybrid functional developed for main group chemistry but also applied to transition metal chemistry⁶. The fact that DFT only optimizes a single determinant has led to the suggestion that systems of multi-reference character are not well-described by DFT³. Wave function theory needs multiple determinants to describe such systems. However, this is less true for DFT, where the density is the fundamental parameter and the single determinant serves a different purpose as density generator, not wave function, as proven by Kohn and Sham⁷; i.e. DFT can describe multi-reference systems accurately when the universal functional is applied to a single Kohn-Sham determinant. However, DFT suffers from a problem of universality because while improvement can be gained by adding mathematical complexity or parameters, there is no *systematic* path toward improvement, except perhaps by using the recently suggested energy-density plots⁸.

Prediction and rational design and improvement of chemical reactions require estimates of the involved bond energies with as little error as possible. To illustrate this, consider a Haber-Bosch process, which involves bonding between a transition metal (most often iron) and N_2 and H_2 , and the subsequent cleavage of these molecules into atomic nitrogen and hydrogen⁹. The errors associated with the computed M-N, N-N, H-H, and M-H bond energies build up to produce a total error in a way that is generally not well accounted for. Errors in the strongest, highly correlated bonds between main-group elements such as CO and N_2 contribute very substantially and up to 100 kJ/mol to these errors, making these strong bonds an “accuracy bottleneck” in theoretical catalysis¹⁰. However, M-L bonds regularly pose even more complex electron correlation effects and may also contribute substantially to the total error. However, we expect that this depends drastically on the type of M-L bond, the d^q configuration of the metal, and the properties of L.

Jensen et al. systematically benchmarked the bond dissociation energies (BDE) of 80 M-L diatomics arguing that these are important data for improving functionals toward d-block transition metal chemistry: They represent the fundamental M-L bonds without complications of solvent effects (experimental data are in gas phase), dispersion (present in larger systems), entropy (they are derived from standard formation enthalpies), and other modulating bonds, and thus probe purely the ability of DFT to model the M-L bond. Subsets of this data set have been substantially scrutinized using various density functionals and correlated methods^{11–14}. Notably, Truhlar et. al.¹¹ studied a subset of 20 of the 80 molecules suggested by Jensen et al., referred to as 3dMLBE20, which are also a subset of the 60 molecules studied in the current paper, and the data set studied by Aoto et al. is very similar but includes some select examples of 4d and 5d transition metals¹⁴.

Jensen et al. discovered a massive general effect of Hartree-Fock (HF) exchange on the M-L bond strength: The strength of a typical M-L bond is overestimated by non-hybrid GGAs, whereas the 20%-HF exchange hybrid B3LYP, the by far most used functional,

under-binds substantially in the 80-system data set¹⁵. Because of this systematic error, a hybrid with 10% HF exchange, e.g. the meta hybrid TPSSh, performs well for the *average* M-L bond of the data set and thus approaches uniform accuracy for the d-block^{16,17}, which may be important when multiple M-L bonds are involved during catalysis and for comparison between metal centers e.g. in catalyst design.

The need for hybrid functionals with modest (10-25%) HF exchange has since then been widely confirmed also for larger systems, showing that the fundamental effect of HF exchange on the M-L bond transfers to the saturated systems: Except in rare cases such as metal-carbon bonds¹⁸, the vast majority of reactions involving M-L bonds become more accurate if some HF exchange is included, and for normal ground state systems this fraction is typically 10-20%, as e.g. in B3LYP with 20% HF exchange^{19,20}, B3LYP* with 15% HF exchange^{21,22}, or TPSSh with 10% HF exchange^{16,23,24}, whereas M-L bond lengths are, interestingly, often accurately described by little or no HF exchange^{15,25}. In the transition states of the reactions, larger amounts of HF exchange is commonly needed due to the self-interaction error of DFT manifesting in diffuse abnormal systems^{26,27}, posing a dilemma that may be partly solved by range-corrected functionals such as CAM-B3LYP²⁸.

This work concerns the identification of M-L accuracy bottlenecks when using DFT. To achieve this, we distinguish between several error types and system dependencies. This is possible if we introduce what we call a “balanced” data set with the same amount of experimental data for all combinations of electronic configurations and atoms. We benchmark 30 representative density functionals (see **Table 1**) to estimate the BDE of 60 diatomic molecules of the 3d-metals (Sc-Zn) with the ligands H, F, Cl, Br, O and S. These systems were chosen because of the availability of experimental data for *all* combinations of the atoms, i.e. they represent a balanced data set for which the performance can be divided into system type. Previous similar studies^{11–13,29–31} should be considered in this context. The main novelty of our study is the use of a balanced dataset studied with a wide range of

modern density functionals of various design types. This enables identification of accuracy bottlenecks without any bias to system type. Our preference for a balanced data set means that some of the experimental data may have a high or no reported uncertainty, and as such it complements the work by Truhlar et al. who selected 20 data points based on small experimental errors¹¹. The 20 ML systems includes nine M-Cl systems, 6 M-H systems, 2 M-S and 3 M-O systems; it includes 4 Zn-L systems but zero with Sc and one with Ti and Ni. Thus, the “3dMLBE20” data set is to 45% testing the metal-chloride bond, and to 25% a test of the M-O/M-S double bond. The neutral M-L diatomics include diverse electron configurations: For example, the Cr and Cu metals dissociate as $4s^13d^5$ and $4s^13d^{10}$ configurations whereas the others dissociate as $4s^23d^q$, which differ in electronic structure, as also seen by the relativistic inert-pair stabilization of $4s^2$ described by Jensen et al.¹⁵ Thus, these configurations should be separated in an error analysis. The halides and hydrides have single-bond character enforcing electronic structures dominated by M^+L^- configurations with 4s participation, whereas the M-O and M-S systems are dominated by the more ionic $M^{2+}L^{2-}$ configuration.

Computational Methods.

The computations were performed with the Turbomole software, version 7.0³² and Gaussian software, version 16³³. We studied 60 neutral diatomic molecules of the M-L type for which BDEs are available in the Handbook of Chemistry and Physics³⁴; the data can be found in **Tables S1 and S2**. The experimental spin states and spin multiplicity used in the computations were obtained from NIST (76 electronic systems in total) as listed in **Tables S3-S5**. The 60 M-L systems include all the 3d transition metals from Sc to Zn bonded to all of the ligands H, F, Cl, Br, O and S. This dataset fundamentally reflects the M-L bond, without complications of solvent effects, dispersion, or other types of bonds that could modulate the bond, and because it is complete for all combinations of M and L, i.e. it is balanced. The M-L systems including N and C studied previously¹⁵ were not included in this study because experimental data are only available for a selection of these systems. Alternative experimental data available in the literature were also analyzed (see below).

We used the geometry-optimized bond lengths of the ground states also used by Jensen, Roos, and Ryde¹⁵ because these were directly validated against the experimental bond lengths with a MAE of 0.02 Å, the best in the study; the effect of geometry due to method choice is substantially smaller than the errors in functionals but comparable to the enthalpy-energy distinction of ~4 kJ/mol, making this distinction less meaningful for these particular diatomic systems¹⁵. All energies were converged to 10⁻⁶ a.u. and the resolution of identity approximation was used to accelerate computation³⁵. The basis set used was def2-QZVPPD for all M (Sc-Zn) and aug-cc-pV5Z for the ligands (H, F, Cl, Br, O, S)^{36,37}. The p-block atoms are more electronegative and thus contain a surplus of electrons and require larger basis sets than the metals. The large basis set ensures that the performance is mainly due to the exchange-correlation functionals and not basis set effects which might differ between systems. Previous work has shown effects for these systems of < 5 kJ/mol moving from triple-zeta-valence to quadruple-zeta-valence basis sets¹⁵, and thus we operate at chemical

accuracy in the chosen basis sets. All atoms should be described by a set of polarization functions, as these are important for describing the various types of M-L bonding¹⁵. The BDE was calculated using equation (1):

$$BDE(M-L) = -E(M-L) + E(M) + E(L) - E_{ZPE}(M-L) - E_{rel}(M-L) + E_{rel}(M) + E_{rel}(L) \quad (1)$$

$BDE(M-L)$ is the BDE for the M-L bond. E_{rel} is the scalar relativistic energy correction previously computed¹⁵ and applied to all electronic systems. Spin-orbit coupling contributions are relatively small for these systems, typically 0-5 kJ/mol with a few exceptions (for some Co and Ni systems it can reach 8-12 kJ/mol)^{11,13}. The scalar-relativistic correction mimics within chemical accuracy the full relativistic corrections mainly because of this³⁸ but are important¹⁵ due to the differential stabilization of the $4s^2$ configurations (inert pairs) of all the M ground states except the $3d^5 4s^1$ state of Cr and the $3d^{10} 4s^1$ state of Cu, thereby making the BDE relatively larger in the latter two cases. The corrections can be seen in **Table S6**. $E_{ZPE}(M-L)$ is the computed zero point energy of the molecule¹⁵ (see **Table S7**) using the BP86 functional. This correction, like the geometry, does not vary significantly due to functional choice and thus was applied throughout. $E(M-L)$ is the single point energy calculated for the diatomic M-L, available in **Tables S8-S37**. $E(M)$ and $E(L)$ are the single-point electronic energies of atoms M and L, respectively, available in **Tables S38-S42**.

Please note that some authors compare to D_0 whereas others compare to D_e , and some correct for enthalpy terms whereas others do not. The experimental data have average errors of ~20 kJ/mol and were derived both from formation enthalpies and from spectroscopic data, the latter subsequently corrected for $3/2 RT$ (~3.7 kJ/mol). Thus, the conversion term between energy and enthalpy at 298 K is smaller than chemical accuracy for these particular systems. Our computed energies are formally at 0 K, corrected for zero-point vibrational energy. The specific use of equilibrium bond lengths at 0 K (vs. 298 K) make this enthalpy-

energy conversion less meaningful and would correspondingly not affect the conclusions of our study.

The signed errors (SE) discussed in this work were calculated by equation 2:

$$SE = BDE(M - L)_{computed} - BDE(M - L)_{experimental} \quad (2)$$

where $BDE(M - L)_{computed}$ is the BDE calculated from eq. 1 while $BDE(M - L)_{experimental}$ is the experimental value from **Table S1**. We also report absolute errors (AE) as the numerical value of the SE, and the mean absolute error (MAE) and mean signed error (MSE) as averages of these two errors across the data. The errors obtained for each method with or without relativistic corrections, using alternative experimental data as explained below, exclusion of outliers, and sub-data sets are tabulated in **Tables S43-S48**. Individual errors for all 30 functionals for all systems are compiled in **Tables S49-S78**.

The 30 studied exchange-correlation functionals are summarized in **Table 1**. They include many popular density functionals⁶ and importantly span across many design types to ensure a large spread in performance². Where possible, these were studied using their keywords in Turbomole, whereas others were studied using the xcfun library module implemented with Turbomole³⁹. MN15, MN15-L, and M06-L were computed using Gaussian 16. We first computed M06-L using Turbomole but noticed a much worse performance vs. the Gaussian version of M06-L, and thus decided to report only the latter. Briefly, local density approximations (LDA) use only the electron density in their description of the energy. Generalized gradient approximations (GGA) include also the gradient of the density. The non-separable gradient approximation (NGA) also depends on the spin (up/down) densities and the reduced gradient of the spin densities in a non-separable way. Meta GGA functionals have contributions from the gradient as well as the Laplacian of the density and/or the kinetic energy density gradient. The hybrid functionals include a fraction of HF exchange; this fraction varies substantially and substantially impacts chemical energies^{18,40}.

Table 1. The 30 exchange-correlation functionals used in this work, their functional type, the amount of Hartree-Fock exchange (if any), and their key references.

Functional	Type	% HF exchange	References
BLYP	GGA	0	41,42
BP86	GGA	0	41,43
PBE	GGA	0	44
BVWN	GGA	0	43,45
B97D	GGA	0	46
OLYP	GGA	0	47,48
OPBE	GGA	0	44,49
PW91	GGA	0	50
RPBE	GGA	0	51
B3LYP	Hybrid GGA	20	5,48,52
PBE0	Hybrid GGA	25	44,53
B3P86	Hybrid GGA	20	41,42
BHLYP	Hybrid GGA	50	54
CAM-B3LYP	Range-separated hybrid	19-65	28
PBE0-10	Hybrid GGA	10	44 and this work
PBEh-3C	Hybrid GGA	42	55
TPSSH	Hybrid meta GGA	10	56
M06	Hybrid meta GGA	27	57
M06-2X	Hybrid meta GGA	54	57
PWLDA	LDA	0	58
SVWN	LSDA	0	45,59
TPSS	Meta GGA	0	56
M06-L	Meta GGA	0	60
B3LYP-5	Hybrid GGA	5	5,48,52 and this work
B2PLYP	Double Hybrid	53	61
PW6B95	Hybrid meta GGA	28	62
B97-1	Hybrid GGA	21	63
B97-2	Hybrid GGA	21	64
MN15	Hybrid meta NGA	44	65
MN15-L	Meta NGA	0	66

Results and Discussion.

The mean signed errors (MSE) and the mean absolute errors (MAE) of the functionals for the full data set are summarized in **Figure 1**, fully corrected for scalar-relativistic and zero-point contributions. **Figure 1A** shows the errors upon comparison to the experimental data from the CRC Handbook of Chemistry & Physics, whereas **Figure 1B** shows the errors calculated using seven alternative experimental BDEs found in the literature. These values for MnH, VCl, CrO, FeH, CoH, ZnO, and ZnS differ substantially and the red values are probably closer to the true values as discussed below. The MAE indicates the numerical precision of each functional, whereas the MSE reveals the systematic tendency of the functional to over- or underestimate the M-L bond strength, and thus both these errors are of interest in the following.

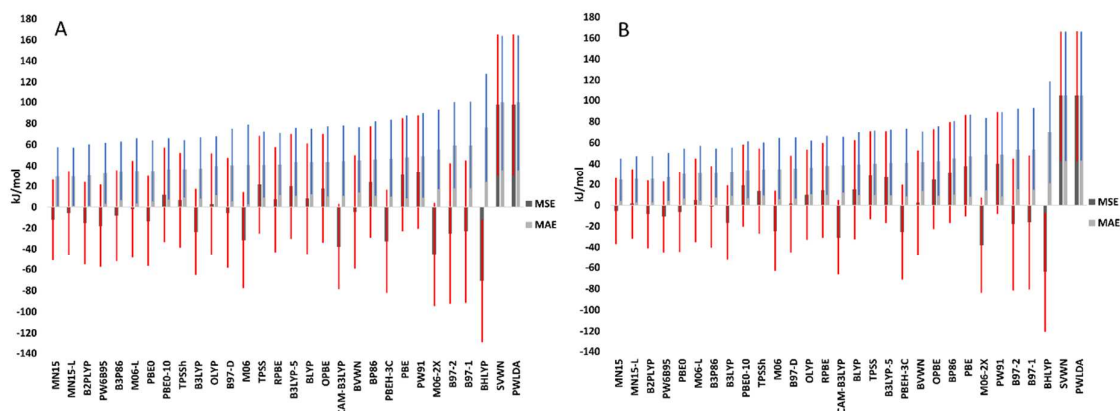


Figure 1. Mean signed error (MSE) and mean absolute error (MAE) for the 30 functionals applied to M-L diatomics; **A)** with data from the Handbook of Chemistry and Physics; **B)** using alternative experimental values for VCl, CrO, MnH, FeH, CoH, ZnO and ZnS (red values in **Table S1**); the red line represents the average \pm the standard deviation of the SE, and the blue line is the same for the AE (tabulated numbers can be found in **Tables S44** and **S45**).

From **Figure 1A** (numerical data in **Table S44**), the MAEs range from 29-100 kJ/mol and the MSEs ranges from -71 (BHLYP) to +98 (PWLDA) kJ/mol. We were also interested in knowing how these errors spread for each functional, i.e. their *precision*; we estimate this by the standard deviation of the SE and AE. From these, we have plotted also the average error +/- the standard deviations as red and blue lines in **Figure 1A** (i.e. each of these bars has a length of two standard deviations). The standard deviations for each functional are found in **Table S44** and range from 39-68 kJ/mol for the SE, and from 28-64 kJ/mol for the AE. The average *reported* (but not true, *vide infra*) experimental uncertainty (**Table S2**) is ~20 kJ/mol for the 48 experimental values where the uncertainty was reported. This brings an interesting concept into play which has not broadly been discussed in DFT benchmarking, namely the accuracy vs. precision of a functional. Generally, the MAE and MSE measure the overall accuracy and precision but not the expected variation from this precision, which is obtained by the standard deviations. **Figure 1** shows importantly that the functionals more or less follow the expected scaling between the magnitude and expected variance in SE, with accurate functionals also having higher precision, i.e. smaller variation in errors.

The top-5 functionals of **Figure 1A** are MN15, MN15-L, B2PLYP, PW6B95 and B3P86. These functionals have MAEs in the range of 29-35 kJ/mol and standard deviations of the AE of 28-30 kJ/mol. A negative value of the MSE corresponds to under-binding and a positive to over-binding. The local functionals, represented by PWLDA and SVWN, overbind massively as is well-known⁶⁷. Interestingly, all the non-hybrid GGAs and to a smaller extent the 10%-hybrids overbind in the data set. It is also notable that we can distinguish the “simple” hybrids as those that are not the double hybrid B2PLYP or the new distinctly parameterized MN15. All the simple hybrids with more than 10% HF exchange underestimate the strength of the M-L bond on average for the data set; in contrast, B2PLYP and MN15 remedy their large HF fractions in two distinct ways, by explicit MP2 correlation or parameterization.

It is also interesting to investigate system-specific HF requirements. Changing from 25% (PBE0) to 10% HF-exchange (PBE0-10) with everything else kept constant leads to a change from -14 kJ/mol under-binding to an over-binding of 12 kJ/mol. This fits well with the above conclusion. Similar observations with B3LYP and BLYP, BP86, and PBE led to the suggestion to use TPSSH with 10% HF exchange for studying M-L bond-forming and bond-breaking processes¹⁶. The impact of using only modest HF-exchange was studied using a customized version of B3LYP with 5% HF-exchange (B3LYP-5). This led to a change from 15 kJ/mol under-binding to 29 kJ/mol over-binding and increased the overall MAE from 37 to 43 kJ/mol (**Table S44**). The best performing GGA functional is OLYP, which has a remarkably low MSE of only 3 kJ/mol but still a MAE of 40 kJ/mol. Thus, OLYP is an excellent choice of non-hybrid GGA functional considering that its energies are computed considerably faster than those of the hybrid functionals.

The MN15 and MN15-L functionals perform best for the general data set. It is also notable that the MN15-L functional has a local form that makes it fast to compute relative to most other functionals; even without considering this, MN15-L is an excellent choice for studying M-L bonds of the type benchmarked here. The excellent performance of MN15 and MN15-L is partly due to the parameterization toward a very large diverse data set that also includes many main group and metal-ligand bond strengths^{65,66}. Thus, care should as always be exercised when using such functionals outside their parameterization range, as shown in a recent independent benchmark⁶⁸. In this context, the similarly excellent performance of B2PLYP and PW6B95 with much fewer parameters is notable.

Very many studies in heterogeneous catalysis use either PBE or its revised versions, exemplified here by RPBE. The RPBE method was introduced to improve adsorption energies of ligands to metals⁵¹. **Figure 1** shows that for the full balanced data set, PBE performs quite poorly, with a substantial bias toward forming too strong M-L bonds by 31 kJ/mol (MAE 48 kJ/mol); this was also noted in earlier work¹⁵. For our dataset, which gives

no preference to any d^q configuration, metal, ligand or bond type of those studied, RPBE is a substantial improvement over PBE as it reduces the over-binding tendency of PBE considerably (MSE 7 kJ/mol; MAE = 41 kJ/mol) (**Table S44**), but less so using the more realistic alternative data (**Table S45**). For this dataset, where all d^q configurations are treated with the same weight, RPBE has a modest over-binding tendency of 7-14 kJ/mol (**Table S44 vs. S45**). These results were obtained with relativistic and zero-point-energy corrections. Had these not been included, as is often the case in surface catalysis, the errors would be considerably larger. Applying RPBE without relativistic correction increases MSE from 7 to 16 kJ/mol (**Table S44 vs. S43**), and if ZPE is ignored the over-binding will increase further by up to 10 kJ/mol for hydrides, but less for heavier ligands binding to metals (**Table S7**).

Figure 1B shows the same comparison as in **Figure 1A** using the alternative data for VCl, CrO, MnH, FeH, CoH, ZnO, and ZnS (marked red in **Table S1**; see **Table S45** for specified errors). The ordering of top-5 has changed a little but not significantly given the similar performance overall. Importantly, both the MAEs and the standard deviations of the errors have been reduced by ~5 kJ/mol using the alternative data set. We explain below why we trust the alternative values. With these data, we reach a target best accuracy of DFT applied to the full, balanced data set of 25 kJ/mol MAE. Similar conclusions are reached if the disputed data are simply removed from comparison (**Figure S1, Table S46**). This should be put in the context of the average experimental error of 20 kJ/mol, which may be a lower bound (see below), i.e. we are close to the limit of accuracy achievable for a diverse, balanced data set. Again, it is notable that the 4s/3d configurations change along the data series, making the data set more challenging than initially meets the eye. Below we investigate if this general performance can be further analyzed in terms of system dependencies.

If we restrict our analysis to the subset of 20 systems of the 3dMLBE20 data set¹¹, we see a remarkable improvement of the MAE compared to the full dataset of **Figure 1 (Table**

S47, Figure S2). The improvement of the MAE is in most cases ~ 10 -15 kJ/mol and possibly relates to the fact that the 3dMLBE20 data set has smaller experimental errors so that comparison is more accurate, and partly to the fact that the 20 ML systems are a relatively simpler and less diverse in their electronic structure than the full, balanced benchmark data set. As mentioned above, 9 of these 20 systems are chlorides. From **Figure S2** it can be seen that the ranking of functionals is similar to that of **Figure 1B**. The best performing functional for the 3dMLBE20 data set is PW6B95, according to our computations with the aug-cc-pV5Z/def2-QZVPP basis set, corrected for scalar-relativistic and zero-point effects, with an estimated uncertainty of ~ 5 kJ/mol in the ranking. It shows a MSE of only -1 kJ/mol and a MAE of 7 kJ/mol. However, even for this carefully selected data set with a tendency to show smaller errors, the standard deviation of the SE is 25-53 kJ/mol, i.e. the precision of DFT remains a major issue.

The 3dMLBE20 dataset but with the values for VH, CrH, FeH and CoH omitted has also been studied in great detail with CC methods by Cheng et al.¹³ A MAE of 10 kJ/mol, MSE of -8 kJ/mol, and STD for SE of 12 kJ/mol was achieved for CCSD(T) using a basis set of similar quality as ours (penta-zeta polarized for the electronegative ligands). For these 16 systems, which are clearly some of the “easiest” of the 60 systems, and which is more than half chlorides, our analysis of functional performance is shown in **Table S48** and **Figure S3**. As expected, errors and standard deviations become even smaller as the data set becomes less chemically diverse, again testifying to the importance of our notion of a balanced data set.

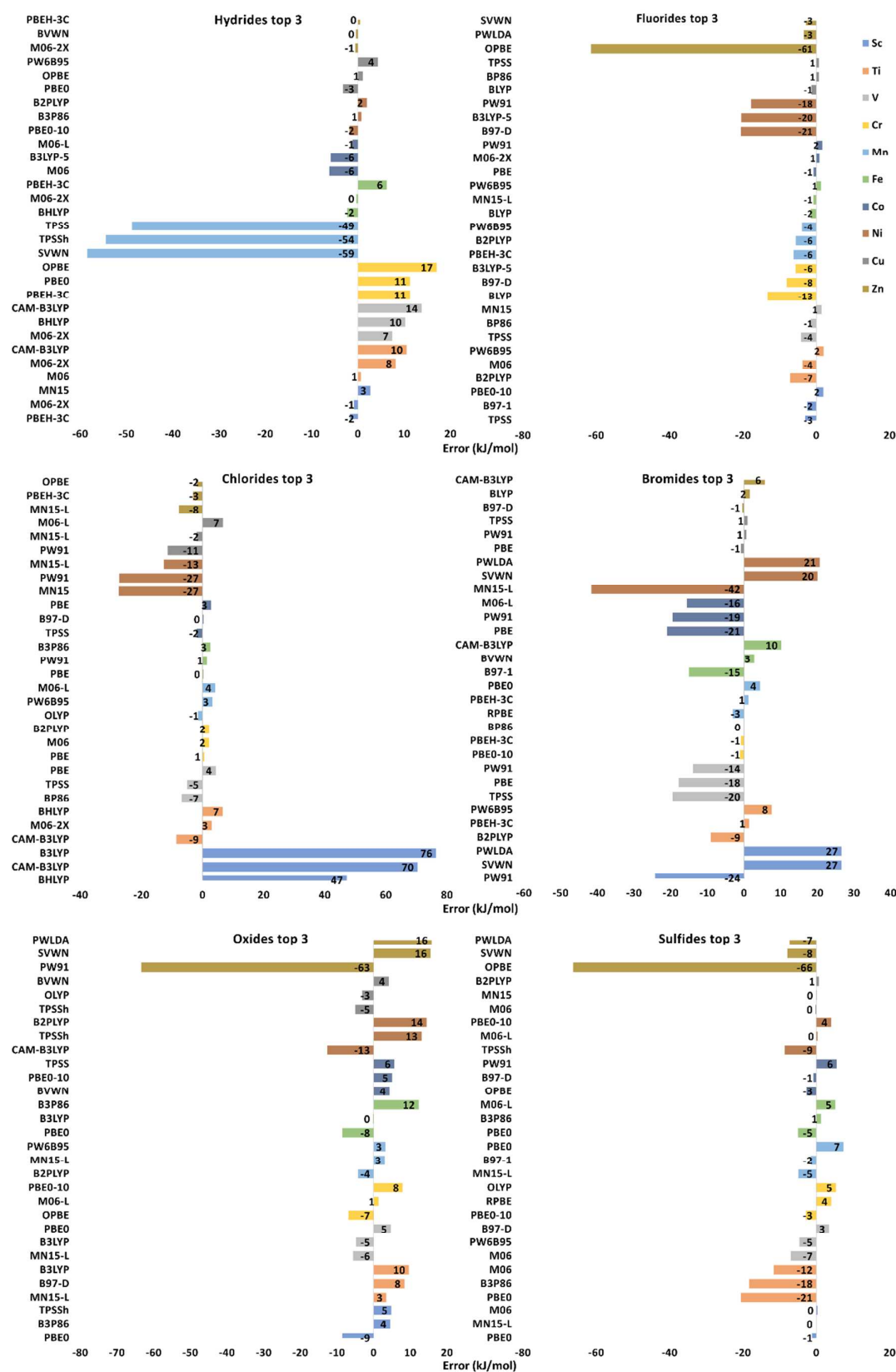


Figure 2. Pathological systems as identified from the errors of the three best-performing functionals for each of the 60 systems with errors in kJ/mol (numbers in **Tables S49-S78**).

Errors Divided into Systems and Choice of Experimental Data. To further dissect system dependencies, **Figure 2** shows the errors of the three most accurate functionals for each of the 60 molecules using the data from the CRC Handbook³⁴. As expected from the overall performance, the hybrid functionals are frequently in the top 3. Six of the 60 studied systems have very large errors even for the best functionals, namely ScCl, MnH, NiBr, ZnF, ZnO and ZnS. Thus **Figure 2** also conveniently indicates questionable experimental data, because it is unlikely that all of such a broad range of density functionals, including known strong underbinders and overbinders, have large errors. Furthermore, there are notable system dependencies that need attention. Below, using **Figure 2** as a guide, we explain why the alternative data in **Figure 1B** are preferred and argue the interesting fact that modern DFT can be used to discard experimental data if compared in the context of a wider data set.

To illustrate this, for ScCl, even the best performing functional BHLYP has an error of 47 kJ/mol, and it comes with a rather large over-binding. This is extremely surprising since BHLYP with 50% HF exchange is expected to be massively under-binding, as also confirmed by the MSE for the entire dataset of -71 kJ/mol (**Table S44**). Thus, the experimental value of 331 kJ/mol for ScCl as already previously stated¹⁵ seems too low, and thus it is reasonable to question the experimental value. Another experimental estimate puts it at ~500 kJ/mol, which is, on the other hand, too large using a similar analysis as the above. Highly correlated methods put it at ~448 kJ/mol⁶⁹.

MnH (having a $^7\Sigma^+$ state) provides another example that also explains why we put less emphasis on the experimentally reported uncertainties than others do¹¹ (although some of these, in all fairness, are adequately estimated, many are probably not). The experimental value from the CRC Handbook³⁴ is 251 kJ/mol. The smallest error with any functional using the Handbook data is -49 kJ/mol for a functional known to overbind (TPSS). This is, together with the similar performance of over-binding functionals, in our experience a strong

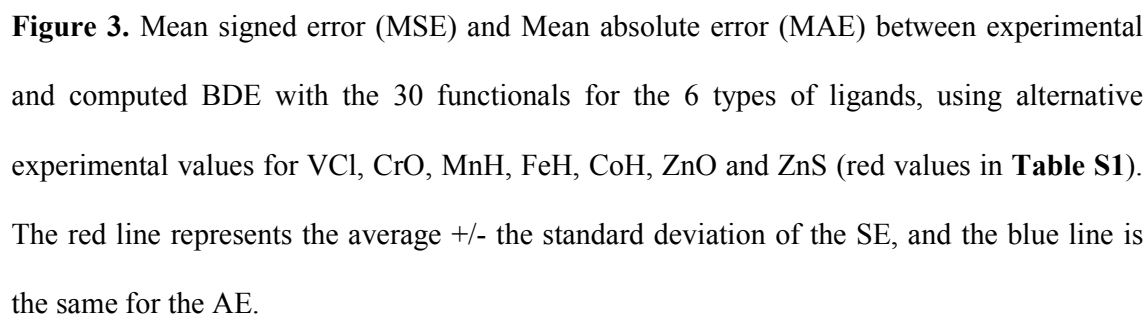
indication that the experimental number is too large. While the experimental uncertainty of MnH is listed as 5 kJ/mol (**Table S2**), an alternative experimental value⁷⁰ (red value in **Table S2**) reads only 126 kJ/mol. This number is much more acceptable in relation to the DFT results and their known systematic errors. Thus, it is not surprising that multi-reference CC reproduces the latter value with good accuracy (10-20 kJ/mol)¹⁴, indicating its essential correctness. Experimental uncertainties may sometimes underestimate true errors that become evident from reproducibility tests: Even if statistical replicate experiments were carried out adequately and in sufficient numbers, they were still performed by a distinct research group in a distinct way at a distinct time with strong underlying correlators.

NiBr, ZnF, ZnO and ZnS have among their top-3 functionals the two LDAs PWLDA and SVWN. It seems highly unlikely that local density functionals predict the BDEs of these particular systems well but fail massively for most other systems in the balanced data set, including those that resemble the “successes”. The MSE for PWLDA and SVWN for the entire dataset is +98 and +97 kJ/mol respectively. This indicates that the experimental values for NiBr, ZnO, ZnS and ZnF are too large. The experimental uncertainty has been reported to be 63 kJ/mol for ZnF and the value for ZnO was simply stated as > 250 kJ/mol. Indeed, there are alternative experimental data for ZnO and ZnS also used by Truhlar et. al.¹¹ which are much lower than the values from the Handbook³⁴. Some of these were derived from the experimental formation enthalpies using vibrational corrections calculated with M06-L, but they should still largely reflect the experimental formation enthalpies as the vibrational corrections are not very method-sensitive, and are thus probably more accurate than the CRC Handbook data for these selected cases.

With these alternative data (marked in red in **Table S1**) the errors for ZnO and ZnS are reduced dramatically, to the range that we expect based on the performance for other systems. Thus we conclude that the values of ZnO and ZnS from the Handbook³⁴ are too large and the alternative data seem accurate. Please note that we can also conclude from this

1 that Aoto et al.¹⁴ only see a very large error for ZnS but not ZnO because they use the right
2 experimental value for ZnO but the wrong experimental value for ZnS; had they used the
3 value of 143 kJ/mol they would have seen that their calculation of ZnS using multireference
4 coupled-cluster is actually accurate, as we expect it to be, and they were correct in asking for
5 a revision of the experimental data point they had used in their benchmark.
6
7
8
9
10
11
12

13 After analyzing the experimental data, we now return to discuss the system
14 dependencies of the DFT performance, deemphasizing the largest bars in **Figure 2** as
15 discussed above. We were particular interested in understanding whether DFT performance is
16 transferable among M-L bonds or subject to large system dependencies, whether the need for
17 HF exchange depends on the system, and if there are any fundamental accuracy bottlenecks
18 once the revised data are taken into account. To show this more clearly, the errors of the
19 functionals were ranked for each type of ligand in **Figure 3**.
20
21
22
23
24
25
26
27
28
29
30
31
32
33
34
35
36
37
38
39
40
41
42
43
44
45
46
47
48
49
50
51
52
53
54
55
56
57
58
59
60



Error Dependencies on Ligand Type. In this work, we were particularly interested in understanding whether there are accuracy bottlenecks that would in particular challenge the use of DFT in catalysis and inorganic chemistry. **Figure 3** shows the MSE and MAE and their respective standard deviations separately for all six ligands (H, F, Cl, Br, O, and S). **Figure 3** immediately reveals that the performance of each functional is very system-dependent. Some of these, in particular the problem of the hydrides, have been noted previously^{12,15}.

The hydrides are notable in that they differ the most from the consensus ranking in **Figure 1**. Thus, BHLYP performs best for the hydrides but on average describes bonding very poorly due to its very large HF exchange percentage, which leads to underestimated M-L bond strengths. BHLYP and PBEh-3C both have very high HF-exchange percentages (50% and 42%) that are not compensated as in B2PLYP. The hydrides with the dominating M^+H^- configuration are characterized by a very polar sigma bond with possible participation or in other cases non-bonding behavior of the 4s orbital on the metal. Some functionals were designed to give almost exact values of -0.5 a.u. for hydrogen, whereas M and MH have not experienced the same favor; this creates an imbalance in the modeled BDE. The hydride resonance form may be prone to self-interaction error of the loosely bound 4s electron, which is probably more non-bonding in the hydrides compared to the halides due to the low energy of the M-L σ molecular orbital. This could be relevant to a wide range of catalytic processes including the Haber-Bosch process mentioned in the introduction. **Figure 3** shows that the hydrides contribute to the accuracy bottleneck because the functionals that normally perform well are challenged.

For the fluorides a complete opposite scenario is seen, which very much justifies our use of balanced data sets: For these, there is a tendency to favor the non-hybrid GGAs or meta functionals (TPSS), whereas the hybrids underbind too much. The hydrides and halides

are all characteristic of forming M-L single bonds with a dominant contribution from the M^+L^- configuration, whereas the MO and MS systems almost invariably form double bonds with a dominant contribution from the $M^{2+}L^{2-}$ configuration. This means that the metal state contains more 4s character in the halides and hydrides, which may explain the difference observed in **Figure 3**. In the halide series F^- , Cl^- , and Br^- , all systems favor a relatively small HF percentage, in most cases 0-10%. To further confirm this, we also studied a customized version of B3LYP with only 5% HF exchange, called B3LYP-5. Although this functional is less accurate for the total data set, it outperforms B3LYP for F, Cl, and Br.

In contrast, for the oxides and sulfides, except for the highly parameterized MN15-L functional, the hybrid functionals dominate completely but at more moderate HF percentages. Thus, the oxides and sulfides appear “average” in the data set in terms of their HF exchange requirements, and detailed analysis reveals that the hydrides and halides behave very distinctly from the group of oxides and sulfides. These three distinct groups of systems average out to a preferred amount of HF exchange of 10-25% but for hydrides it is markedly higher and for halides it is somewhat smaller. Thus, the performance of any functional towards a data set, such as e.g. the 3dMLBE20 subset studied by Truhlar and co-workers¹¹, which is 45% chlorides, should be considered in this context. It is interesting that the excellent performance of the MN15 and MN15-L functionals breaks with the HF exchange requirements seen for less parameterized functionals, i.e. the HF exchange requirements can be compensated by the functional form.

System-dependent HF exchange is a challenge to theoretical catalysis, both homogenous and heterogeneous, where ligands bind to and dissociate from a metal catalyst. Interestingly, the range-corrected CAM-B3LYP, which performs relatively poorly for the halides, performs well for both hydrides and oxides, indicating possible ways forward when such functionals can be applied. It is also interesting that RPBE performs average for all ligand types, i.e. it may display good cancellation of error in real applications, probably

Sc

MSE
MAE

B3LYP B2PLYP TPSSH PBE0 PW6B95 B3P86 B97-D MN15-L M06 MN15 PBE0-10 B97-2 B97-1 CAM-B3LYP BVWN RPBE M06-2X PBEH-3C TPSS OLP NREL-M06L OPBE B3LYP-5 PBE PW91 BHLYP SVWN PWLDA

Ti

MSE
MAE

M06 B2PLYP MN15 PW6B95 B97-D MN15-L CAM-B3LYP PBE0 PBEH-3C B3LYP M06-L B3P86 M06-2X OLYP BVWN B97-1 B97-2 BLYP RPBE BHLYP TPSS PBE0-10 TPSSH B3LYP-5 OPBE BPBE PW91 PWLDA

V

MSE
MAE

B3LYP BLYP BP86 PBE PBE0 TPSSH PBEH-3C BVWN PWLDA B97-D B3P86 CAM-B3LYP M06-2X M06-L OLYP OPBE PBE0-10 PBEH-3C PW91 RPBE SVWN B3LYP-5 B2PLYP PW6B95 B97-1 B97-2 MN15 MN15-L

Cr

MSE
MAE

PBE0-10 TPSSH MN15 B2PLYP OPBE CAM-B3LYP M06 B3LYP B3P86 OLYP PW6B95 MN15-L RPBE TPSS PBE BP86 PBE0 PW91 B3LYP-5 BLYN BVWN M06-2X M06-L PBEH-3C B97-D BHLYP B97-2 SVWN

Mn

MSE
MAE

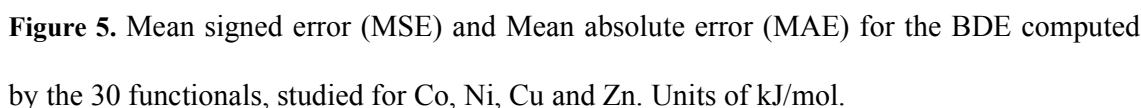
PW6B95 MN15-L B2PLYP MN15 PBE0 B3LYP PBEH-3C B3P86 M06-L OLYP CAM-B3LYP BLYP B97-D B3LYP-5 BVWN TPSSH PBE0-10 RPBE M06 M06-2X PBEH-3C BP86 OPBE B97-1 TPSS PBE B97-2 PW91 PWLDA SVWN

Fe

MSE
MAE

MN15-L MN15 M06-L B2PLYP PW6B95 B3LYP PBE0 B3P86 CAM-B3LYP PBEH-3C TPSSH OLYP RPBE BVWN PBE0-10 OPBE M06 BLYP TPSS B97-D B3LYP-5 BP86 M06-2X PBE B97-2 B97-1 PW91 BHLYP SVWN

23



As seen from **Figures 4** and **5**, a general observation is the consistent over-binding of the local density functionals PWLDA and SVWN, which are almost similar in performance

as they should be by design (PWLDA used the Perdew-Wang exchange functional instead of the Slater exchange, but otherwise they are similar). Another general observation is the consistent under-binding of BHLYP and M06-2X with 50% or more HF exchange, as expected. A third general conclusion is that although the ranking of functionals change with metal type (see below), the errors of the best functionals are generally of similar magnitude, i.e. there are no distinctly difficult cases for DFT as a whole, except perhaps for Sc which has distinctly the largest bulk errors and fluctuations in performance.

Moving beyond the local density approximation, for the early-mid transition metals in Figure 4, there is a notable system dependent performance of M06, being a very good functional for early transition metals Sc, Ti, V, and Cr (top-6) but falling to average for Mn and Fe, and for the late metals Co-Zn, as seen in **Figure 5**; accordingly, for Zn it is one of the worst functionals. Thus, performance of the M06 functionals is very system-sensitive in a way that can not be easily predicted but can be somewhat systematized as described above.

For the early-mid transition metals (**Figure 4**), a consistent observation is that hybrid functionals perform best and non-hybrids tend to overbind. It is remarkable that this tendency changes for the late transition metals (Figure 5) such that commonly used GGAs perform quite well, although 10%-HF exchange hybrids are probably more accurate. We can conclude that the need for HF exchange is reduced from ~20% to ~10% along the period, although these numbers are modified by other ingredients of the functionals. Again we note the excellent performance of B2PLYP, MN15-L, and MN15 breaking with this requirement by either inclusion of exact MP2 correlation energy or specific parameterization to counter the high (in MN15) or zero (in MN15-L) HF exchange. Accordingly, B3LYP is an excellent choice for early d-block but a poor choice for late transition metals; this difference is consistent across all six early-middle and all four late transition metals. To study many metals more broadly with a single, transferable functional, for example multi-metal catalysts, lower HF percentages are required such as the customized 10% HF version of PBE0 or the 10%

meta hybrid TPSSh, consistent with its previous good performance on average across the d-block^{16,17}. One interpretation is that DFT does not capture well an intrinsic increased tendency to bind more strongly toward the right of the transition series, an effect that could relate to the increased effective nuclear charge because a remarkably similar effect is seen for the strong bonds of main group atoms¹⁰. Because of this unexplained but important role of effective nuclear charge, the revised RPBE, which reduces the over-binding tendency of PBE, is mainly an advantage for the early-mid transition metals and not very much for the late transition metals (Figure 5), i.e. there is a metal-dependent effect of the relative performance of RPBE vs. PBE due to the phenomenon described above.

DFT Description of Trends in Bonding. Usually, benchmark studies mainly discuss the signed and absolute errors of the functionals, which provide information on the systematic over- or under-binding tendency, i.e. the accuracy, as well as the general numerical accuracy of the functionals. Above, we argued that in some cases, the precision of a functional (as measured by standard deviations of errors) may also be interesting, as it does not always correlate with the accuracy. In addition to these three descriptors, we also argue that the linear trend prediction is an important property of a functional, in particular because most studies in theoretical chemistry are performed with some comparison in mind; otherwise, theoretical chemistry is rarely very useful. Accordingly, a benchmark of the trend prediction capability of functionals should be of interest.

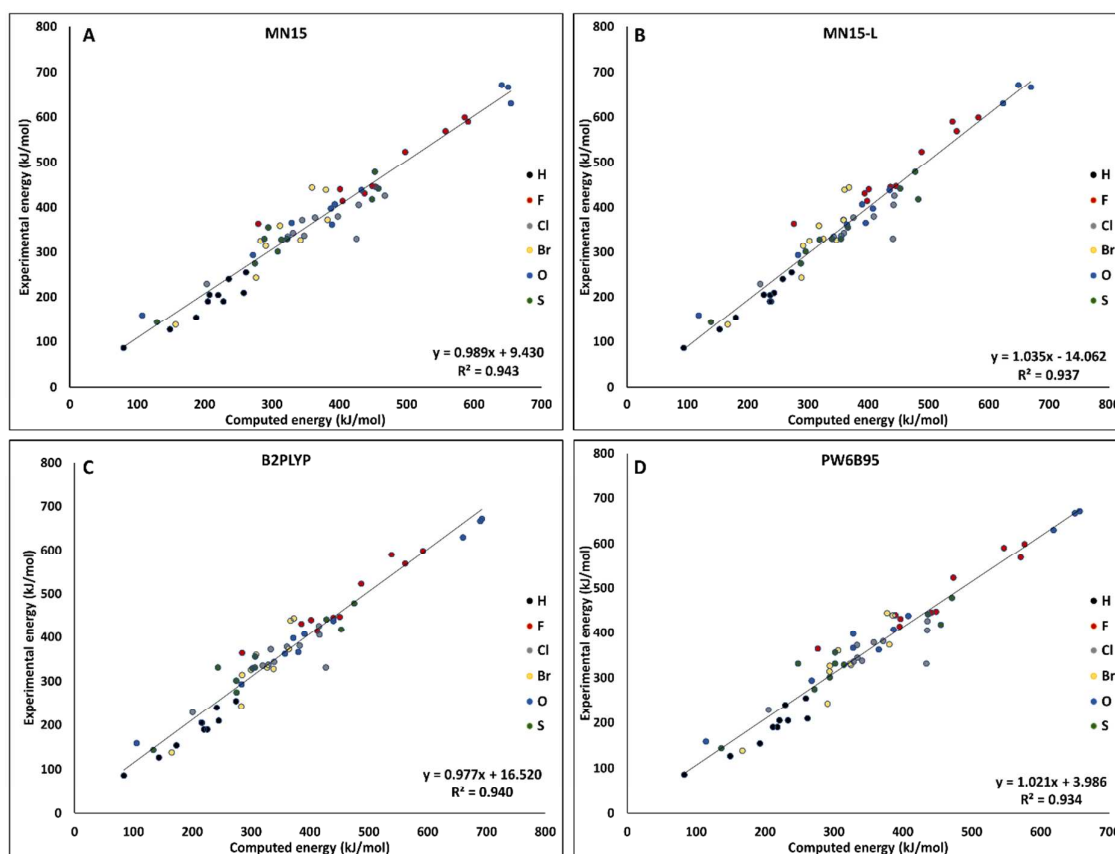


Figure 6. Linear correlation between computed and experimental BDEs for the four functionals with the lowest MAE for all 60 M-L systems using the revised experimental data: A) MN15; B) MN15-L; C) B2PLYP; D) PW6B95.

Figure 6 shows the linear relationship between computed and experimental BDEs for the four overall best-performing functionals in this study: MN15 (**Figure 6A**), MN15L (**Figure 6B**), B2PLYP (**Figure 6C**), and PW6B95 (**Figure 6D**), using our preferred experimental data (**Table S1** using the red numbers). The corresponding plots for all functionals can be found in Supporting Information, **Figures S4-S33**. Generally, we observe very high linearity with all functionals, with R^2 values up to 0.94, but we note that differences in R^2 of 0.05 may be significant. Importantly, all the best functionals exhibit very high R^2 values (0.93-0.94). With a freely varying linear regression equation, the intersection with the vertical axis ranges from -14 to +17 kJ/mol, which implies that all four functionals in **Figure**

6 interpolate well to the limit of zero bonding; many other functionals do not do so (**Figures S4-S33**). When shown as here, a positive value of intersection implies a constant non-scalable contribution to under-binding that should on average be added to the functional. The best functionals also have excellent inclination coefficients of 0.98-1.04; the inclination indicates that the computed bond strength is well-balanced across the bond strength regime from weak to strong M-L bonds. A value smaller than 1 implies over-binding of the functional which scales linearly with the bond strength. Thus, we conclude from our analysis that each functional has a constant non-scalable and a bond strength-scalable contribution to its errors in modeling bond strengths.

In Supporting Information, **Figures S4-S33**, similar plots for all functionals are given. The GGA non-hybrid functionals such as BLYP (**Figure S5**) show imbalances in trend prediction again with a constant contribution of 34 kJ/mol and a bond-strength scalable factor of 0.87. For BP86, these are 21 kJ/mol and 0.89, and for PBE they are 24 kJ/mol and 0.89, i.e. quite similar for all GGAs. Thus, an M-L BDE can be better estimated from such a GGA functional by scaling down the computed BDE by a factor of 0.89 and adding 26 kJ/mol. Such correction (after proper optimization) may be a decent simple correction to a PBE calculation but will, as explained above, be system-dependent, although system-specific scale factors could be envisioned. Similarly, local DFT methods such as PWLDA could be massively improved by simply scaling the computed BDE by a factor of 0.74 (**Figure S12**) and adding only a small constant (e.g. 13 kJ/mol). Considering the speed of these functionals this may be useful in some circumstances. There are also large differences in the scatter of the functionals, related to the precision as discussed above. Thus PBE0-10 is an example of a customized functional with a favorably smaller scatter than both PBE0 and PBE (**Figure S22** vs. **Figure S7/S8**). As a final remark, comparison of the trend prediction of revised RPBE vs. PBE (**Figure S25** vs. **Figure S7**) reveals that RPBE has mainly improved over PBE by reducing the bond-strength scalable contribution to over-binding (0.89 for RPBE vs. 0.84 for

PBE) whereas the constant non-scalable contribution to over-binding remains similar for both functionals and of the order of 25 kJ/mol.

Conclusions. M-L bonds are the fundamental unit of inorganic chemistry and are routinely formed and broken in chemical reactions; we want to understand these bond strengths as well as possible. We have studied a balanced data set of 60 diatomic ML systems and used this data set to discover several new features of DFT applied to these M-L bonds the functionals that have not been reported before despite several benchmark studies of related systems^{11–15}.

Some main observation are: 1) The functionals PW6B95, MN15, MN15-L and the double hybrid B2PLYP on average produce the smallest errors for the combined data set. 2) For GGA hybrids, the performance across the d-block M-L bonds in general is best with 10-25% HF exchange. 3) However, the general performance hides substantial system dependencies that appear consistently both with respect to metal and ligand. 4) In case of ligands, hydrides prefer larger HF exchange fractions of up to 50%; we discuss that the hydrides represent specifically challenging systems for DFT possibly due to self-interaction errors of the non-bonding 4s electron. In contrast, halides prefer low HF exchange of 0-10%, whereas the $M^{2+}L^{2-}$ oxides and sulfides without 4s participation prefer 10-20 % HF exchange. 5) For metals, the most pronounced and consistent observation is that early-mid d-block metals prefer 10-20% HF exchange, whereas late transition metals (Co, Ni, Cu, and Zn) are best described by 0-10 % HF exchange. These tendencies are consistent for the groups of metals and for the various functionals, and thus significant. 6) Apparent DFT performance for M-L bonds are very data-set dependent, and these dependencies should be carefully considered when modeling processes where M-L bonds are broken and formed. These observations strongly support our notion of using a “balanced” data set. 7) We also analyze and stress the importance of the precision, rather than just the accuracy, of DFT. We measure

the precision by the standard deviation of the errors and find that it often correlates with the accuracy. 8) We analyze the relative performance and system dependencies of PBE vs. its revised version RPBE and show that RPBE is mainly an advantage for specific systems where the over-binding tendency of PBE are most pronounced. 9) Finally, we stress the importance of trend prediction by DFT as measured by linear regression plots and show how to interpret the linear regression-line equation data. Specifically, we find that there are errors in functionals that are constant non-scalable and others that scale with the bond strength of the computed bond. We identify a remarkable, general tendency of DFT to intrinsically underestimate the bond strengths of late vs. early transition series, illustrated by the reduced need for HF exchange towards the right of the period; this tendency correlates with increased effective nuclear charge as also seen for main group bonds¹⁰ and may be one of the most important accuracy bottlenecks of current DFT. We hope that our conclusions may be of relevance to future considerations in the study of theoretical catalysis and the development of improved density functionals.

Acknowledgements. We acknowledge the use of the Steno Cluster at DTU Chemistry, originally funded by The Danish Council for Independent Research | Natural sciences (FNU), grant # 272-08-0041.

Supporting Information available.

The Supporting information file contains the experimental data set for the 60 ML systems, electronic energies of all computed systems with all functionals, errors and standard deviations, and linear correlation plots for all functionals. This material is available free of charge via the Internet at <http://pubs.acs.org>.

References.

- (1) Becke, A. D. Perspective: Fifty Years of Density-Functional Theory in Chemical Physics. *J. Chem. Phys.* **2014**, *140* (18), 18A301.
- (2) Perdew, J. P.; Schmidt, K. Jacob's Ladder of Density Functional Approximations for the Exchange-Correlation Energy. *AIP Conf. Proc.* **2001**, *577* (1), 1–20.
- (3) Mardirossian, N.; Head-Gordon, M. Thirty Years of Density Functional Theory in Computational Chemistry: An Overview and Extensive Assessment of 200 Density Functionals. *Mol. Phys.* **2017**, *115* (19), 2315–2372.
- (4) Bauschlicher, C. W. A Comparison of the Accuracy of Different Functionals. *Chem. Phys. Lett.* **1995**, *246* (1), 40–44.
- (5) Becke, A. D. Density-functional Thermochemistry. III. The Role of Exact Exchange. *J. Chem. Phys.* **1993**, *98* (7), 5648–5652.
- (6) Swart, M.; Bickelhaupt, F. M.; Duran, M. DFT2016 Poll. **2016**.
- (7) Kohn, W.; Sham, L. J. Self-Consistent Equations Including Exchange and Correlation Effects. *Phys. Rev.* **1965**, *140* (4A), A1133--A1138.
- (8) Kepp, K. P. Energy vs. Density on Paths toward More Exact Density Functionals. *Phys. Chem. Chem. Phys.* **2018**, *20* (11), 7538–7548.
- (9) Vojvodic, A.; Medford, A. J.; Studt, F.; Abild-Pedersen, F.; Khan, T. S.; Bligaard, T.; Nørskov, J. K. Exploring the Limits: A Low-Pressure, Low-Temperature Haber–Bosch Process. *Chem. Phys. Lett.* **2014**, *598*, 108–112.
- (10) Kepp, K. P. Trends in Strong Chemical Bonding in C₂, CN, CN[−], CO, N₂, NO, NO⁺,

- and O₂. *J. Phys. Chem. A* **2017**, *121* (47), 9092–9098.
- (11) Xu, X.; Zhang, W.; Tang, M.; Truhlar, D. G. Do Practical Standard Coupled Cluster Calculations Agree Better than Kohn–Sham Calculations with Currently Available Functionals When Compared to the Best Available Experimental Data for Dissociation Energies of Bonds to 3d Transition Metals? *J. Chem. Theory Comput.* **2015**, *11* (5), 2036–2052.
- (12) Zhang, W.; Truhlar, D. G.; Tang, M. Tests of Exchange–Correlation Functional Approximations against Reliable Experimental Data for Average Bond Energies of 3d Transition Metal Compounds. *J. Chem. Theory Comput.* **2013**, *9* (9), 3965–3977.
- (13) Cheng, L.; Gauss, J.; Ruscic, B.; Armentrout, P. B.; Stanton, J. F. Bond Dissociation Energies for Diatomic Molecules Containing 3d Transition Metals: Benchmark Scalar-Relativistic Coupled-Cluster Calculations for 20 Molecules. *J. Chem. Theory Comput.* **2017**, *13* (3), 1044–1056.
- (14) Aoto, Y. A.; de Lima Batista, A. P.; Köhn, A.; de Oliveira-Filho, A. G. S. How to Arrive at Accurate Benchmark Values for Transition Metal Compounds: Computation or Experiment? *J. Chem. Theory Comput.* **2017**, *13* (11), 5291–5316.
- (15) Jensen, K. P.; Roos, B. O.; Ryde, U. Performance of Density Functionals for First Row Transition Metal Systems. *J. Chem. Phys.* **2007**, *126*, 14103.
- (16) Jensen, K. P. Bioinorganic Chemistry Modeled with the TPSSh Density Functional. *Inorg. Chem.* **2008**, *47*, 10357–10365.
- (17) Jensen, K. P. Metal-Ligand Bonds of Second and Third Row D-Block Metals Characterized by Density Functional Theory. *J. Phys. Chem. A* **2009**, *113*, 10133–10141.
- (18) Jensen, K.; Ryde, U. Theoretical Prediction of the Co–C Bond Strength in Cobalamins.

- J. Phys. Chem. A* **2003**, *155*, 7539–7545.
- (19) Frenking, G.; Fröhlich, N. The Nature of the Bonding in Transition-Metal Compounds. *Chem. Rev.* **2000**, *100* (2), 717–774.
- (20) Siegbahn, P. E. M.; Blomberg, M. R. A. Transition-Metal Systems in Biochemistry Studied by High-Accuracy Quantum Chemical Methods. *Chem. Rev.* **2000**, *100* (2), 421–438.
- (21) Reiher, M.; Salomon, O.; Hess, B. A. Reparameterization of Hybrid Functionals Based on Energy Differences of States of Different Multiplicity. *Theor. Chem. Acc.* **2001**, *107* (1), 48–55.
- (22) Reiher, M. Theoretical Study of the Fe (phen)₂(NCS)₂ Spin-Crossover Complex with Reparametrized Density Functionals. *Inorg. Chem.* **2002**, *41* (25), 6928–6935.
- (23) Jensen, K. P.; Cirera, J. Accurate Computed Enthalpies of Spin Crossover in Iron and Cobalt Complexes. *J. Phys. Chem. A* **2009**, *113*, 10033–10039.
- (24) Kepp, K. P.; Dasmeh, P. Effect of Distal Interactions on O₂ Binding to Heme. *J. Phys. Chem. B* **2013**, *117*, 3755–3770.
- (25) Bühl, M.; Kabrede, H. Geometries of Transition-Metal Complexes from Density-Functional Theory. *J. Chem. Theory Comput.* **2006**, *2* (5), 1282–1290.
- (26) Perdew, J. P.; Zunger, A. Self-Interaction Correction to Density-Functional Approximations for Many-Electron Systems. *Phys. Rev. B* **1981**, *23* (10), 5048–5079.
- (27) Wasserman, A.; Nafziger, J.; Jiang, K.; Kim, M.-C.; Sim, E.; Burke, K. The Importance of Being Inconsistent. *Annu. Rev. Phys. Chem.* **2017**, *68* (1), 555–581.
- (28) Yanai, T.; Tew, D. P.; Handy, N. C. A New Hybrid Exchange–correlation Functional Using the Coulomb-Attenuating Method (CAM-B3LYP). *Chem. Phys. Lett.* **2004**, *393*

- (1), 51–57.
- (29) Minenkov, Y.; Chermak, E.; Cavallo, L. Troubles in the Systematic Prediction of Transition Metal Thermochemistry with Contemporary Out-of-the-Box Methods. *J. Chem. Theory Comput.* **2016**, *12* (4), 1542–1560.
- (30) Jiang, W.; Laury, M. L.; Powell, M.; Wilson, A. K. Comparative Study of Single and Double Hybrid Density Functionals for the Prediction of 3d Transition Metal Thermochemistry. *J. Chem. Theory Comput.* **2012**, *8* (11), 4102–4111.
- (31) Determan, J. J.; Poole, K.; Scalmani, G.; Frisch, M. J.; Janesko, B. G.; Wilson, A. K. Comparative Study of Nonhybrid Density Functional Approximations for the Prediction of 3d Transition Metal Thermochemistry. *J. Chem. Theory Comput.* **2017**, *13* (10), 4907–4913.
- (32) Turbomole 7.0. University of Karlsruhe and Forschungszentrum Karlsruhe GmbH 2012, p available from <http://www.turbomole.com>.
- (33) Frisch, M. J.; Trucks, G. W.; Schlegel, H. B.; Scuseria, G. E.; Robb, M. A.; Cheeseman, J. R.; Scalmani, G.; Barone, V.; Petersson, G. A.; Nakatsuji, H.; et al. Gaussian 16, Revision A.03. 2016.
- (34) Rumble, J. R.; Rumble, J. *CRC Handbook of Chemistry and Physics, 98th Edition*; CRC Handbook of Chemistry and Physics; CRC Press LLC, 2017.
- (35) Eichkorn, K.; Treutler, O.; Öhm, H.; Häser, M.; Ahlrichs, R. Auxiliary Basis Sets to Approximate Coulomb Potentials. *Chem. Phys. Lett.* **1995**, *240* (4), 283–290.
- (36) Dunning, T. H. Gaussian Basis Sets for Use in Correlated Molecular Calculations. I. The Atoms Boron through Neon and Hydrogen. *J. Chem. Phys.* **1989**, *90* (2), 1007–1023.
- (37) Weigend, F.; Ahlrichs, R. Balanced Basis Sets of Split Valence, Triple Zeta Valence

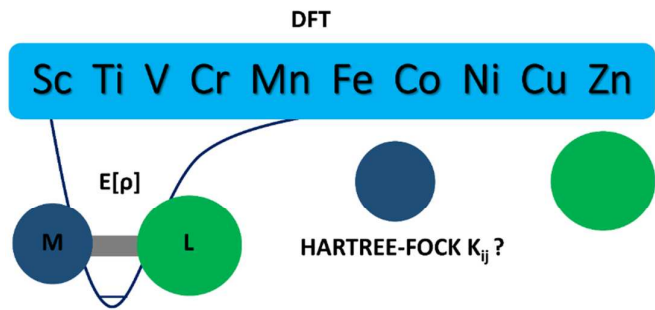
- and Quadruple Zeta Valence Quality for H to Rn: Design and Assessment of Accuracy. *Phys. Chem. Chem. Phys.* **2005**, 7 (18), 3297–3305.
- (38) Kepp, K. P. Theoretical Study of Spin Crossover in 30 Iron Complexes. *Inorg. Chem.* **2016**, 55 (6), 2717–2727.
- (39) Ekström, U.; Visscher, L.; Bast, R.; Thorvaldsen, A. J.; Ruud, K. Arbitrary-Order Density Functional Response Theory from Automatic Differentiation. *J. Chem. Theory Comput.* **2010**, 6 (7), 1971–1980.
- (40) Salomon, O.; Reiher, M.; Hess, B. A. Assertion and Validation of the Performance of the B3LYP* Functional for the First Transition Metal Row and the G2 Test Set. *J. Chem. Phys.* **2002**, 117 (10), 4729–4737.
- (41) Perdew, J. P. Density-Functional Approximation for the Correlation Energy of the Inhomogeneous Electron Gas. *Phys. Rev. B* **1986**, 33 (12), 8822–8824.
- (42) Becke, A. D. Density-Functional Exchange-Energy Approximation with Corrects Asymptotic-Behavior. *Phys. Rev. A* **1988**, 38 (6), 3098–3100.
- (43) Becke, A. D. Density-Functional Exchange-Energy Approximation with Correct Asymptotic Behavior. *Phys. Rev. A* **1988**, 38 (6), 3098–3100.
- (44) Perdew, J. P.; Burke, K.; Ernzerhof, M. Generalized Gradient Approximation Made Simple. *Phys. Rev. Lett.* **1996**, 77 (18), 3865.
- (45) Vosko, S. H.; Wilk, L.; Nusair, M. Accurate Spin-Dependent Electron Liquid Correlation Energies for Local Spin Density Calculations: A Critical Analysis. *Can. J. Phys.* **1980**, 58 (8), 1200–1211.
- (46) Grimme, S. Semiempirical GGA-Type Density Functional Constructed with a Long-Range Dispersion Correction. *J. Comput. Chem.* **2006**, 27 (15), 1787–1799.

- (47) Handy, N. C.; Cohen, A. J. Left-Right Correlation Energy. *Mol. Phys.* **2001**, *99* (5), 403–412.
- (48) Lee, C.; Yang, W.; Parr, R. G. Development of the Colle-Salvetti Correlation-Energy Formula into a Functional of the Electron Density. *Phys. Rev. B* **1988**, *37* (2), 785–789.
- (49) Cohen, A. J.; Handy, N. C. Assessment of Exchange Correlation Functionals. *Chem. Phys. Lett.* **2000**, *316* (1), 160–166.
- (50) Perdew, J. P.; Chevary, J. A.; Vosko, S. H.; Jackson, K. A.; Pederson, M. R.; Singh, D. J.; Fiolhais, C. Atoms, Molecules, Solids, and Surfaces: Applications of the Generalized Gradient Approximation for Exchange and Correlation. *Phys. Rev. B* **1992**, *46* (11), 6671–6687.
- (51) Hammer, B.; Hansen, L. B.; Nørskov, J. K. Improved Adsorption Energetics within Density-Functional Theory Using Revised Perdew-Burke-Ernzerhof Functionals. *Phys. Rev. B* **1999**, *59* (11), 7413.
- (52) Stephens, P. J.; Devlin, F. J.; Chabalowski, C. F.; Frisch, M. J. Ab Initio Calculation of Vibrational Absorption and Circular Dichroism Spectra Using Density Functional Force Fields. *J. Phys. Chem.* **1994**, *98* (45), 11623–11627.
- (53) Adamo, C.; Barone, V. Toward Reliable Density Functional Methods without Adjustable Parameters: The PBE0 Model. *J. Chem. Phys.* **1999**, *110* (13), 6158–6170.
- (54) Becke, A. D. A New Mixing of Hartree–Fock and Local Density functional Theories. *J. Chem. Phys.* **1993**, *98* (2), 1372–1377.
- (55) Grimme, S.; Brandenburg, J. G.; Bannwarth, C.; Hansen, A. Consistent Structures and Interactions by Density Functional Theory with Small Atomic Orbital Basis Sets. *J. Chem. Phys.* **2015**, *143* (5), 54107.
- (56) Staroverov, V. N. Comparative Assessment of a New Nonempirical Density

- Functional: Molecules and Hydrogen-Bonded Complexes. *J. Chem. Phys.* **2003**, *119* (23).
- (57) Zhao, Y.; Truhlar, D. G. The M06 Suite of Density Functionals for Main Group Thermochemistry, Thermochemical Kinetics, Noncovalent Interactions, Excited States, and Transition Elements: Two New Functionals and Systematic Testing of Four M06-Class Functionals and 12 Other Function. *Theor. Chem. Acc.* **2008**, *120* (1–3), 215–241.
- (58) Perdew, J. P.; Wang, Y. Accurate and Simple Analytic Representation of the Electron-Gas Correlation Energy. *Phys. Rev. B* **1992**, *45* (23), 13244.
- (59) Slater, J. C. *Quantum Theory of Molecular and Solids. Vol. 4: The Self-Consistent Field for Molecular and Solids*; McGraw-Hill: New York, 1974.
- (60) Zhao, Y.; Truhlar, D. G. A New Local Density Functional for Main-Group Thermochemistry, Transition Metal Bonding, Thermochemical Kinetics, and Noncovalent Interactions. *J. Chem. Phys.* **2006**, *125* (19), 194101.
- (61) Grimme, S. Semiempirical Hybrid Density Functional with Perturbative Second-Order Correlation. *J. Chem. Phys.* **2006**, *124* (3), 34108.
- (62) Zhao, Y.; Truhlar, D. G. Design of Density Functionals That Are Broadly Accurate for Thermochemistry, Thermochemical Kinetics, and Nonbonded Interactions. *J. Phys. Chem. A* **2005**, *109* (25), 5656–5667.
- (63) Hamprecht, F. A.; Cohen, A. J.; Tozer, D. J.; Handy, N. C. Development and Assessment of New Exchange-Correlation Functionals. *J. Chem. Phys.* **1998**, *109* (15), 6264–6271.
- (64) Wilson, P. J.; Bradley, T. J.; Tozer, D. J. Hybrid Exchange-Correlation Functional Determined from Thermochemical Data and Ab Initio Potentials. *J. Chem. Phys.* **2001**,

- 115 (20), 9233–9242.
- (65) Yu, H. S.; He, X.; Li, S. L.; Truhlar, D. G. MN15: A Kohn-Sham Global-Hybrid Exchange-Correlation Density Functional with Broad Accuracy for Multi-Reference and Single-Reference Systems and Noncovalent Interactions. *Chem. Sci.* **2016**, 7 (8), 5032–5051.
- (66) Yu, H. S.; He, X.; Truhlar, D. G. MN15-L: A New Local Exchange-Correlation Functional for Kohn–Sham Density Functional Theory with Broad Accuracy for Atoms, Molecules, and Solids. *J. Chem. Theory Comput.* **2016**, 12 (3), 1280–1293.
- (67) Kepp, K. P. Consistent Descriptions of Metal–ligand Bonds and Spin-Crossover in Inorganic Chemistry. *Coord. Chem. Rev.* **2013**, 257 (1), 196–209.
- (68) Mardirossian, N.; Head-Gordon, M. How Accurate Are the Minnesota Density Functionals for Noncovalent Interactions, Isomerization Energies, Thermochemistry, and Barrier Heights Involving Molecules Composed of Main-Group Elements? *J. Chem. Theory Comput.* **2016**, 12 (9), 4303–4325.
- (69) Kardahakis, S.; Mavridis, A. First-Principles Investigation of the Early 3d Transition Metal Diatomic Chlorides and Their Ions, $\text{ScCl}^{0,\pm}$, $\text{TiCl}^{0,\pm}$, $\text{VCl}^{0,\pm}$, and $\text{CrCl}^{0,\pm}$. *J. Phys. Chem. A* **2009**, 113 (24), 6818–6840.
- (70) Sunderlin, L. S.; Armentrout, P. B. Reactions of manganese(1+) with Isobutane, Neopentane, Acetone, Cyclopropane and Ethylene Oxide. Bond Energies for MnCH_2^+ , MnH , and MnCH_3 . *J. Phys. Chem.* **1990**, 94 (9), 3589–3597.

Table of Content Graphic



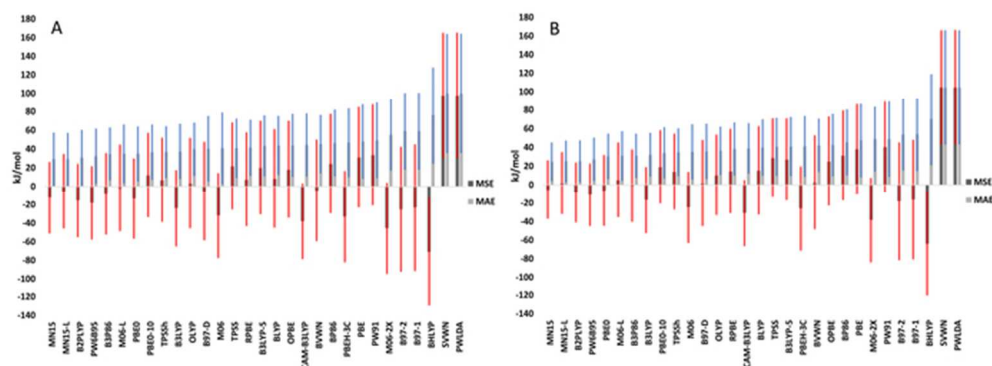


Figure 1

59x21mm (300 x 300 DPI)

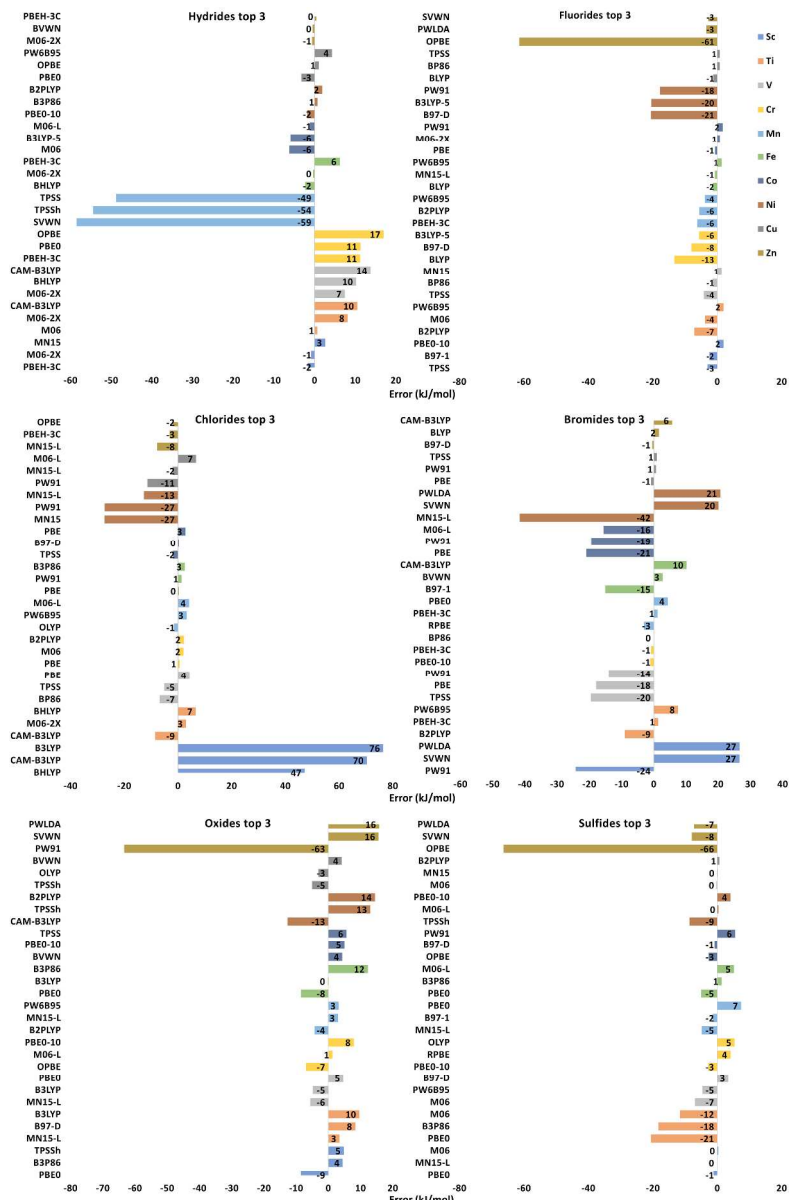


Figure 2

427x658mm (300 x 300 DPI)

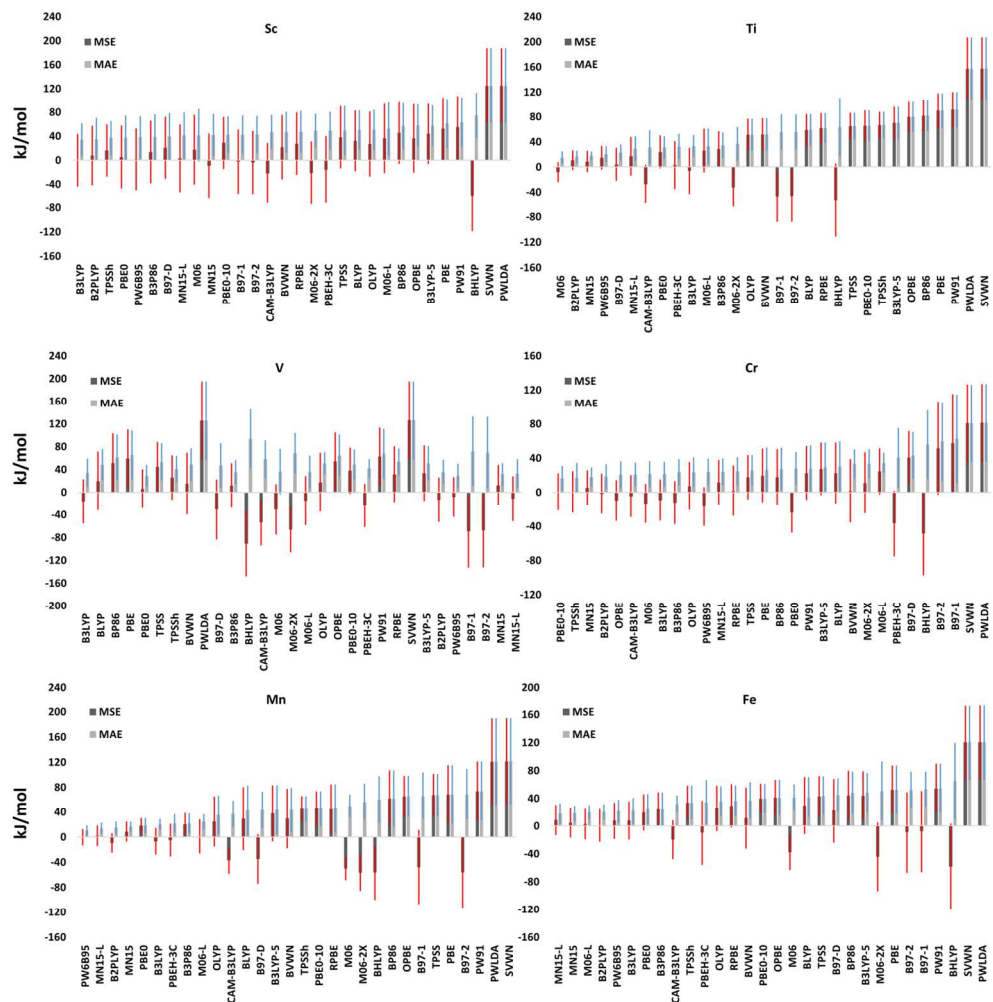
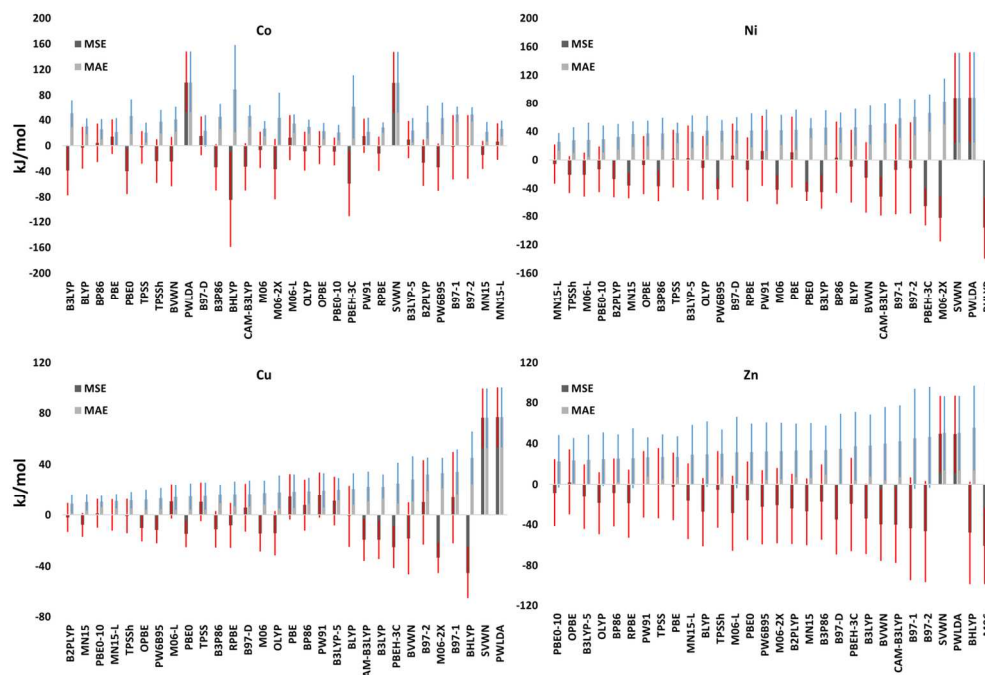


Figure 4

134x135mm (300 x 300 DPI)



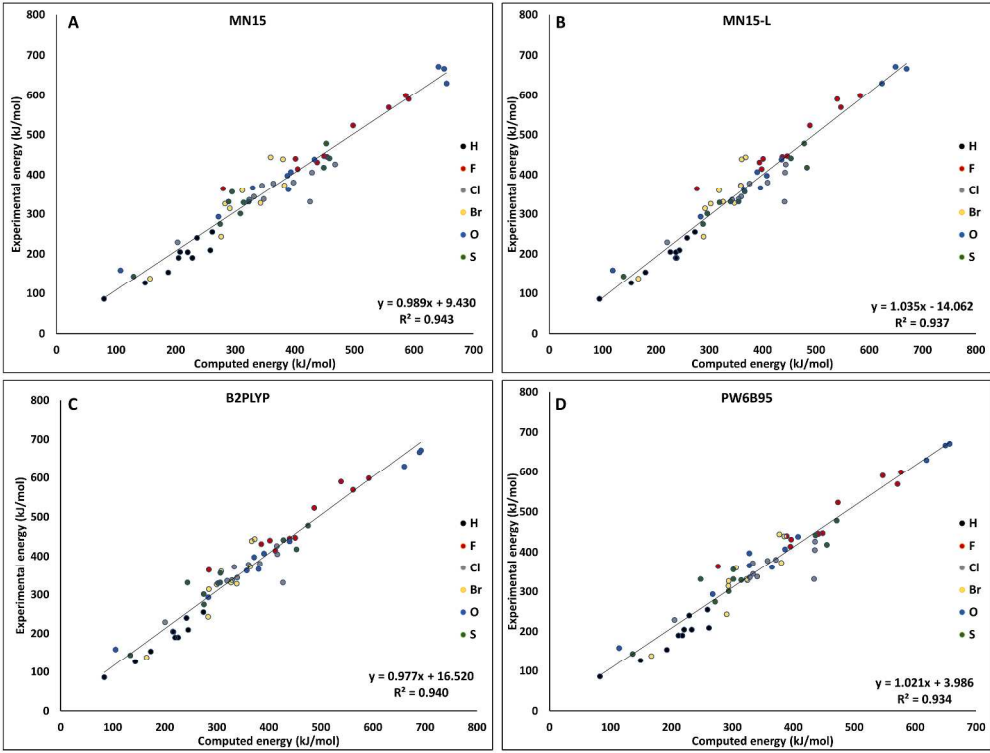
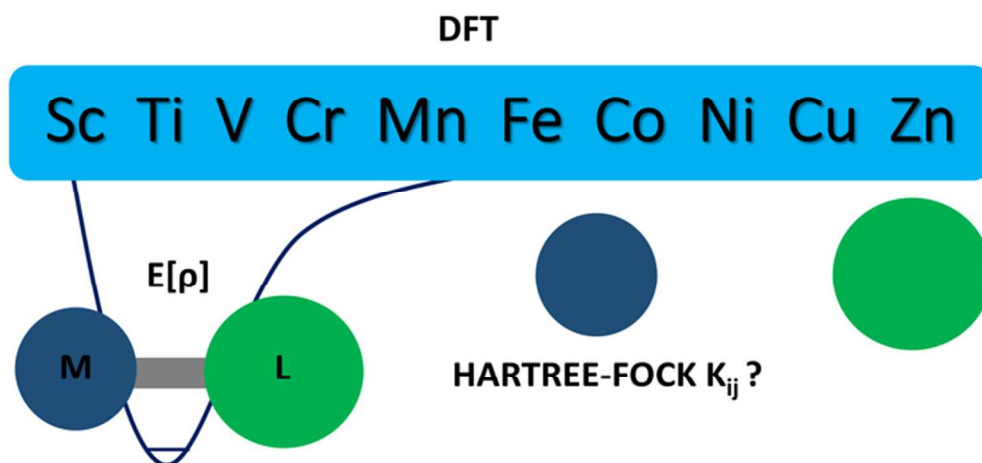


Figure 6

344x259mm (300 x 300 DPI)



TOC figure

63x29mm (300 x 300 DPI)